Versatile DNA damage detection by the global genome nucleotide excision repair protein XPC

Deborah Hoogstraten[1], Steven Bergink[1], Vincent H. M. Verbiest[1], Martijn S. Luijsterburg[3], Bart Geverts[2], Anja Raams[1], Christoffel Dinant[1,2], Jan H. J. Hoeijmakers[1], Wim Vermeulen[1,*] and Adriaan B. Houtsmuller[2,*]

[1]Department of Cell Biology and Genetics and [2]Department of Pathology (Josephine Nefkens Institute), Erasmus MC Rotterdam, P.O. Box 2040, 3000 CA Rotterdam, The Netherlands
[3]Swammerdam Institute for Life Sciences, University of Amsterdam, Kruislaan 318, 1098 SM Amsterdam, The Netherlands
*Authors for correspondence (e-mail: w.vermeulen@erasmusmc.nl; a.houtsmuller@erasmusmc.nl)

Journal of Cell Science 121, 2972 (2008) doi:10.1242/jcs.03502

There was an error published in the e-press version of *J. Cell Sci.* **121**, 2850-2859.

In the e-press version of this paper, Adriaan B. Houtsmuller (a.houtsmuller@erasmusmc.nl) was not acknowledged as a corresponding author.

The authors apologise for this mistake.

Versatile DNA damage detection by the global genome nucleotide excision repair protein XPC

Deborah Hoogstraten[1], Steven Bergink[1], Vincent H. M. Verbiest[1], Martijn S. Luijsterburg[3], Bart Geverts[2], Anja Raams[1], Christoffel Dinant[1,2], Jan H. J. Hoeijmakers[1], Wim Vermeulen[1,*] and Adriaan B. Houtsmuller[2,*]

[1]Department of Cell Biology and Genetics and [2]Department of Pathology (Josephine Nefkens Institute), Erasmus MC Rotterdam, P.O. Box 2040, 3000 CA Rotterdam, The Netherlands
[3]Swammerdam Institute for Life Sciences, University of Amsterdam, Kruislaan 318, 1098 SM Amsterdam, The Netherlands
*Authors for correspondence (e-mail: w.vermeulen@erasmusmc.nl; a.houtsmuller@erasmusmc.nl)

Accepted 3 June 2008
Journal of Cell Science 121, 2850-2859 Published by The Company of Biologists 2008
doi:10.1242/jcs.031708

Summary

To investigate how the nucleotide excision repair initiator XPC locates DNA damage in mammalian cell nuclei we analyzed the dynamics of GFP-tagged XPC. Photobleaching experiments showed that XPC constantly associates with and dissociates from chromatin in the absence of DNA damage. DNA-damaging agents retard the mobility of XPC, and UV damage has the most pronounced effect on the mobility of XPC-GFP. XPC exhibited a surprising distinct dynamic behavior and subnuclear distribution compared with other NER factors. Moreover, we uncovered a novel regulatory mechanism for XPC. Under unchallenged conditions, XPC is continuously exported from and imported into the nucleus, which is impeded when NER lesions are present. XPC is omnipresent in the nucleus, allowing a quick response to genotoxic stress. To avoid excessive DNA probing by the low specificity of the protein, the steady-state level in the nucleus is controlled by nucleus-cytoplasm shuttling, allowing temporally higher concentrations of XPC in the nucleus under genotoxic stress conditions.

Supplementary material available online at
http://jcs.biologists.org/cgi/content/full/121/17/2850/DC1

Key words: DNA binding, DNA repair, Live cell reaction kinetics

Introduction

Nucleotide excision repair (NER) is a versatile DNA repair process, which removes a wide variety of intrastrand lesions that cause helical distortion including UV-induced cyclobutane pyrimidine dimers (CPD) and pyrimidine (6-4) pyrimidone photoproducts [(6-4)PP] (Gillet and Scharer, 2006). The biological significance of functional NER is evident from the clinical features observed in patients suffering from the inherited NER-deficient syndrome xeroderma pigmentosum (XP). Individuals carrying a mutation in one of the seven XP genes (*XPA* to *XPG*) exhibit severe cutaneous symptoms, including extreme UV sensitivity and sun-induced pigmentation anomalies and most importantly a >2000-fold increase in the occurrence of skin cancer.

Two subpathways exist within NER, differing in their mode of damage recognition (Gillet and Scharer, 2006). Transcription-coupled nucleotide excision repair (TC-NER) focuses on transcription-blocking lesions located in the transcribed strand of active genes, whereas global genome nucleotide excision repair (GG-NER) eliminates lesions located anywhere in the genome. TC-NER is initiated by lesion-stalled RNA polymerase whereas both the UV-damaged DNA-binding protein (UV-DDB) complex and the XPC-hHR23B-Cen2 heterotrimeric complex (hereafter named XPC) cooperatively initiate GG-NER (Chu and Chang, 1988; Sugasawa et al., 1998; Wakasugi et al., 2001). Both subpathways funnel into the 'core' NER reaction, which comprises three additional steps: (1) open complex formation and lesion verification; (2) dual incision on either side of the damage to excise an oligonucleotide of 25-30 bases containing the lesion; and (3) gap-filling DNA synthesis and ligation. The DNA around the lesion is melted by the transcription factor IIH (TFIIH) and this open DNA intermediate is stabilized by the replication protein A (RPA) and the NER-specific factor XPA, which are important for proper orientation of the two endonucleases that conduct the dual incision, ERCC1/XPF and XPG. The pre-incision complex contains TFIIH, XPA, RPA and the two endonucleases, but not XPC (Riedl et al., 2003; Wakasugi and Sancar, 1998).

UV-DDB is probably the first factor to bind DNA lesions within GG-NER (Luijsterburg et al., 2007; Wakasugi et al., 2002). The presence of UV-DDB is not strictly required for XPC to bind, although it severely enhances recruitment to 6-4(PP) and is crucial for CPD repair (Alekseev et al., 2005; Moser et al., 2005). However, functional XPC is essential to initiate GG-NER, both in vitro and in intact cells (Sugasawa et al., 1998; Venema et al., 1990; Volker et al., 2001). Purified XPC displays high affinity for undamaged single- and double-stranded DNA (Batty et al., 2000; Masutani et al., 1994), preferentially binds to DNA with various lesions (Reardon et al., 1996) and even to small bubble structures with or without a lesion (Sugasawa et al., 2001). Nevertheless, dual incision was only observed when damage was present in the bubble, suggesting that, after binding of XPC to a locally destabilized helix site, the presence of the injured base is verified by additional NER-specific factors prior to dual incision.

XPC probes sites in the genomic DNA that exhibit a thermodynamically unfavorable configuration (Dip et al., 2004; Gunz et al., 1996), for example, helical distortions that are due to DNA damage. It was shown that XPC recognizes single-stranded configurations and binds to the complementary undamaged strand (Buterin et al., 2005; Maillard et al., 2007). Recent structural studies on a part of the yeast XPC ortholog Rad4 further confirm this XPC-binding mode (Min and Pavletich, 2007). This feature also explains the extraordinary broad diversity of lesions recognized by XPC (ranging from UV-induced lesions to AAF-adducts and

mismatches), since this undamaged non-paired strand is the only common structure within these further structurally unrelated lesions (Maillard et al., 2007). DNA bending as a consequence of this partly unpaired region is stabilized by the XPC (Janicijevic et al., 2003). However, the manner by which XPC finds a lesion in the vast excess of undamaged DNA in the enormous mammalian genome is not clear. DNA-binding proteins are thought to locate target sites by two possible mechanisms (reviewed by Halford and Szczelkun, 2002): (1) proteins could slide along the DNA, i.e. a one-dimensional linear diffusion along the DNA contour, alternatively, (2) translocation of proteins might occur through three-dimensional space, via diffusion and multiple dissociation-reassociation events on the genome.

In order to study the spatiotemporal nuclear distribution of the XPC protein and to determine how this protein is targeted to DNA lesions in intact living cells, we tagged XPC with green fluorescent protein (GFP). Using confocal microscopy and applying various photobleaching techniques, we investigated XPC-GFP mobility in both untreated and UV-irradiated cells, and measured its kinetic engagement with the NER machinery. Previous similar studies on other NER factors, ERCC1/XPF (Houtsmuller et al., 1999), TFIIH (Hoogstraten et al., 2002), XPA (Rademakers et al., 2003), XPG (Zotter et al., 2006) and DDB2 (the GG-NER-specific subunit of UV-DDB) (Luijsterburg et al., 2007), revealed that most NER factors move freely through the nucleus in the absence of large amounts of NER-inducing lesions and became temporarily bound (immobile) to chromatin after UV irradiation (inducing NER lesions). Surprisingly, both the mobility parameters and kinetic engagement of XPC-GFP in NER are considerably different from the other core NER factors.

Moreover, XPC appears to be the focal point of NER regulation at different levels: by a p53-dependent transcriptional induction (Adimoolam and Ford, 2002; Garinis et al., 2005), stabilization by binding to HR23B (Lommel et al., 2002; Ng et al., 2003), by post-translational ubiquitylation, which increases lesion binding affinity (Sugasawa et al., 2005) and by SUMOylation (Wang et al., 2005), which is involved in proteasomal XPC degradation (Wang et al., 2007). Here, we provide further evidence for an additional novel mode of regulating NER activity – reduced nuclear-cytoplasmic shuttling in response to UV irradiation, which temporarily increases the XPC steady-state level in the nucleus.

Results

Generation and characterization of a cell line stably expressing XPC-GFP

To study the spatiotemporal distribution in living cells, we tagged XPC protein at its C-terminus with GFP and additional C-terminal His_6 and HA tags. The fusion gene (*XPC-GFP*) was stably expressed in SV40-immortalized fibroblasts derived from an XP group C patient (XP4PA-SV cells) carrying a 2 bp deletion in the *XPC* gene, creating a frame shift at position 1483 and the introduction of a premature stop codon (Daya-Grosjean et al., 1987). Stable XPC-GFP-expressing cells were isolated in which the mean expression level was comparable with the level of endogenously expressed non-tagged XPC in NER-proficient fibroblasts (Fig. 1A, compare lanes 1 and 3). UV-survival experiments revealed that XPC-GFP corrected the UV-hypersensitivity of XP4PA-SV40 cells to the level of NER-proficient cells that were tested in parallel (Fig. 1B). The performance of XPC-GFP expressed at physiologically relevant levels indicated that these cells are suitable for the study of its dynamic behavior. In the quantitative imaging experiments described below, we took care to only use cells expressing XPC-GFP at physiologically relevant levels as judged by comparative immunofluorescence (Rademakers et al., 2003).

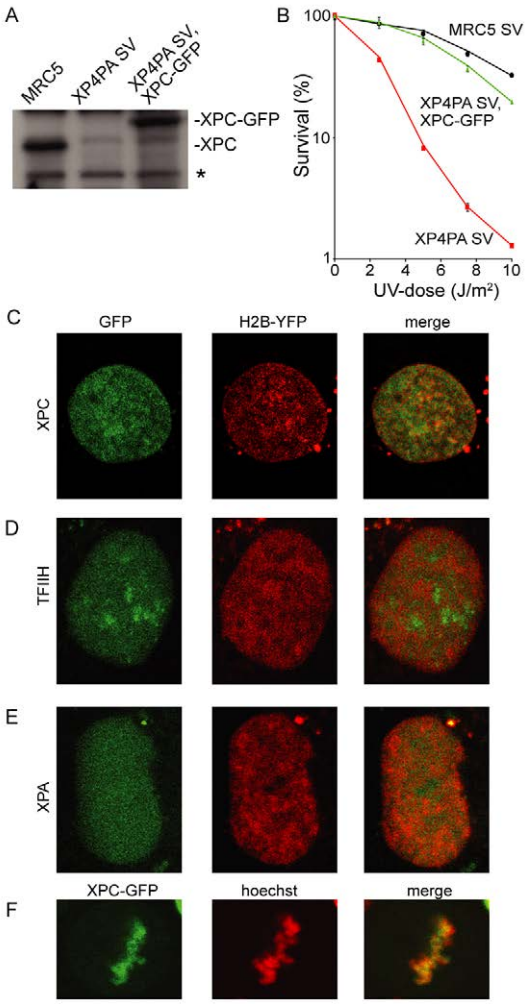

Fig. 1. Characterization of the nuclear distribution of GFP-tagged XPC, XPA and TFIIH in living cells. (A) Immunoblot of whole cell extracts of MRC5 (lane 1), XP4PA SV (lane 2) and population of XP4PA SV cells stably expressing XPC-GFP (lane 3) probed with anti-XPC polyclonal antibodies. The asterisk shows a background band that can serve as a loading control. (B) UV survival of MRC5, XP4PA SV and XP4PA SV cells stably expressing XPC-GFP. The log of the percentage of survival is plotted against the dose of UV-C (J/m^2). (C) Confocal image of a cell stably expressing XPC-GFP (left panel) and transiently expressing H2B-YFP (middle). The merged image is shown in the right panel. (D) A cell stably expressing XPB-GFP (left panel) and transiently expressing H2B-YFP (middle). (E) A cell stably expressing GFP-XPA (left panel) and transiently expressing H2B-YFP (middle). (F) Mitotic cell expressing XPC-GFP. Left panel, GFP fluorescence; middle, Hoechst 33342 staining of DNA; right, merged image.

High-resolution confocal imaging showed that XPC-GFP is predominantly nuclear in living cells, as observed in previously reports (van der Spek et al., 1996; Volker et al., 2001). However, in contrast to the other NER factors, XPC-GFP is non-homogeneously distributed within nuclei (Fig. 1C, left panel). Interestingly, XPC-GFP largely colocalizes with the characteristic heterogeneous pattern of chromatin in interphase nuclei of cultured mammalian cells, visualized using YFP-tagged histone 2B (Kanda et al., 1998) (Fig. 1C, middle and right panels). This indicates that

XPC-GFP is ubiquitous in nuclei and enriched in more condensed chromatin areas. This distribution contrasts with that of other NER factors, such as XPA (Fig. 1E) (Rademakers et al., 2003), which in general are completely homogeneously distributed, except for TFIIH, which also shows accumulations in the nucleolus (Fig. 1D) (Hoogstraten et al., 2002; Verschure et al., 2003). A striking association with the highly condensed metaphase chromosomes was observed in dividing living (Fig. 1F) and fixed cells (van der Spek et al., 1996), consistent with a high affinity of XPC for chromatin. Interestingly, XPC is also different in this respect from other NER factors, which were excluded from condensed chromosomes (data not shown).

The colocalization with condensed mitotic chromatin (Fig. 1F) provided further evidence that XPC has access to and associates with chromatin even at the highest level of condensation, corroborating previous reports that average-sized proteins are not excluded from dense chromatin or chromosomes (Chen et al., 2005; Verschure et al., 2003). In addition, the relatively high level of XPC-GFP fluorescence colocalizing with heterochromatin, indicates that XPC-GFP is not only able to access the condensed part of the genome, as do TFIIH and XPA, but in contrast to these other NER proteins, is also retained there. Recently, we found that DDB2 (subunit of the UV-DDB complex) also localizes to interphase and mitotic chromatin (Luijsterburg et al., 2007) but only upon UV-C irradiation, not in unchallenged cells.

Mobility of XPC-GFP in living mammalian fibroblasts

The inhomogeneous distribution of XPC-GFP suggests that this protein preferentially resides in dense chromatin regions and argues for binding to chromatin in unchallenged cells. To investigate the dynamic distribution of XPC-GFP and compare it with the mobility of other NER factors, we applied photobleaching using different variants of fluorescence recovery after photobleaching (FRAP) (Houtsmuller and Vermeulen, 2001).

FRAP experiments consistently showed that the nuclear mobility of XPC-GFP was surprisingly slow compared with that of GFP-XPA, TFIIH-GFP (a much larger 10-subunit protein complex) (Fig. 2A), (Hoogstraten et al., 2002; Rademakers et al., 2003) and other NER factors (data not shown) (Houtsmuller et al., 1999; van den Boom et al., 2004; Zotter et al., 2006). The mobility of XPC was probably reduced because of interaction with chromatin, since XPC FRAP curves fitted best to FRAP curves generated by Monte Carlo simulation (see Materials and Methods), in which freely diffusing molecules (D_{eff}=7.3±0.5 μm^2/second) very frequently and very transiently interact with immobile elements in an ellipsoid volume (55±8% being immobilized for 310±62 mseconds). The FRAP curves obtained form GFP-XPA fitted best to simulation-generated curves of free diffusion (D_{eff}=11.8±3.7 μm^2/second) (Rademakers et al., 2003), whereas TFIIH fitted best to slower diffusion (D_{eff}=6±2 μm^2/second) and a less transient immobile fraction (22.5±12% for 830±40 mseconds) probably because of its involvement in transcription initiation (Hoogstraten et al., 2002).

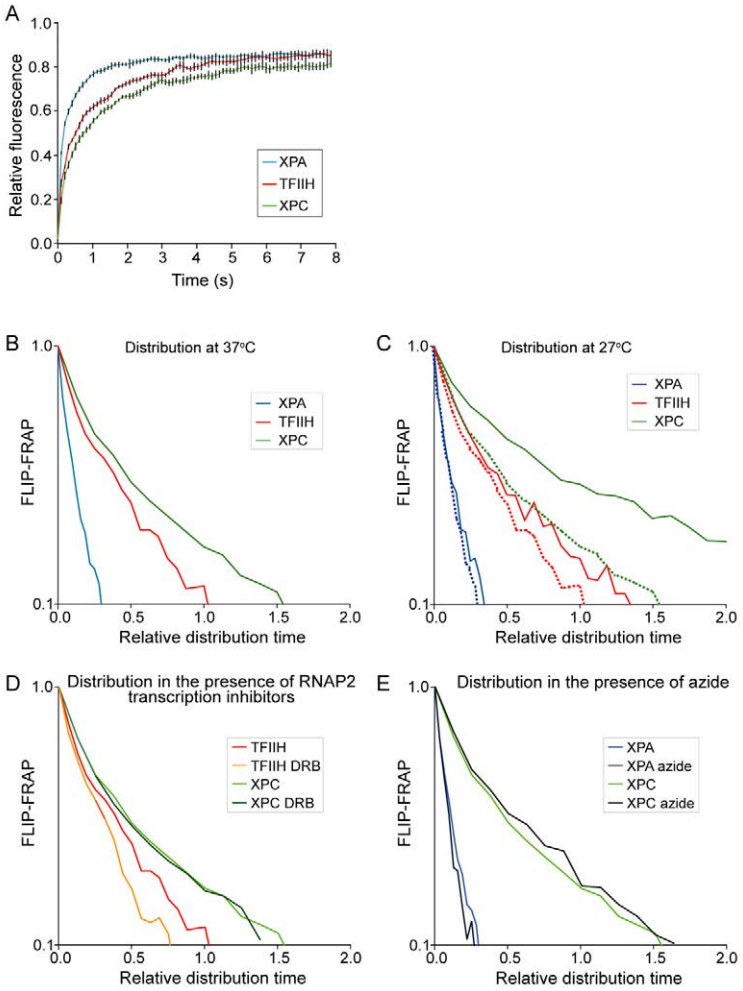

Fig. 2. Dynamics of XPC-GFP, TFIIH-GFP and GFP-XPA. (A) FRAP analysis of untreated GFP-XPA (blue line), XPB-GFP (red line) and XPC-GFP (green line) expressing cells. Error bars represent two times the s.e.m. based on a single experiment, *n*=24. Note that these experiments were repeated at least three times and consistently showed similar mobility differences. (B) Simultaneous FLIP-FRAP analysis on cells expressing GFP-XPA (blue line), XPB-GFP (red line) and XPC-GFP (green line) at 37°C. (C) Simultaneous FLIP-FRAP analysis on cells expressing GFP-XPA (blue line), XPB-GFP (red line) and XPC-GFP (green line) at 27°C. The curves (dashed) obtained at 37°C are also shown. (D) Simultaneous FLIP-FRAP analysis on cells expressing XPB-GFP (red lines) and XPC-GFP (green lines) in the presence and absence of DRB, an RNAP2 transcription inhibitor. (E) Simultaneous FLIP-FRAP analysis on GFP-XPA (blue lines) and XPC-GFP (green lines) expressing cells in the presence and absence of sodium azide.

The reduced mobility of XPC-GFP was confirmed using an alternative FRAP approach in which we determined the mobility of XPC-GFP by monitoring the entire nucleus by FRAP/FLIP (Hoogstraten et al., 2002), yielding a fluorescence redistribution time 1.5 times longer than that of TFIIH (Fig. 2C). Interestingly, the mobility of XPC-GFP was significantly slower when FRAP/FLIP was performed at 27°C instead of 37°C (Fig. 2D). This temperature shift did not significantly affect the mobility of GFP-XPA, as can be expected for a molecule in which the mobility is mainly determined by diffusion (Hoogstraten et al., 2002; Rademakers et al., 2003), but the shift in temperature also slowed down TFIIH-GFP (Fig. 2D). This can be explained by the engagement of TFIIH in transcription initiation, which requires temperature-sensitive enzymatic steps (Hoogstraten et al., 2002).

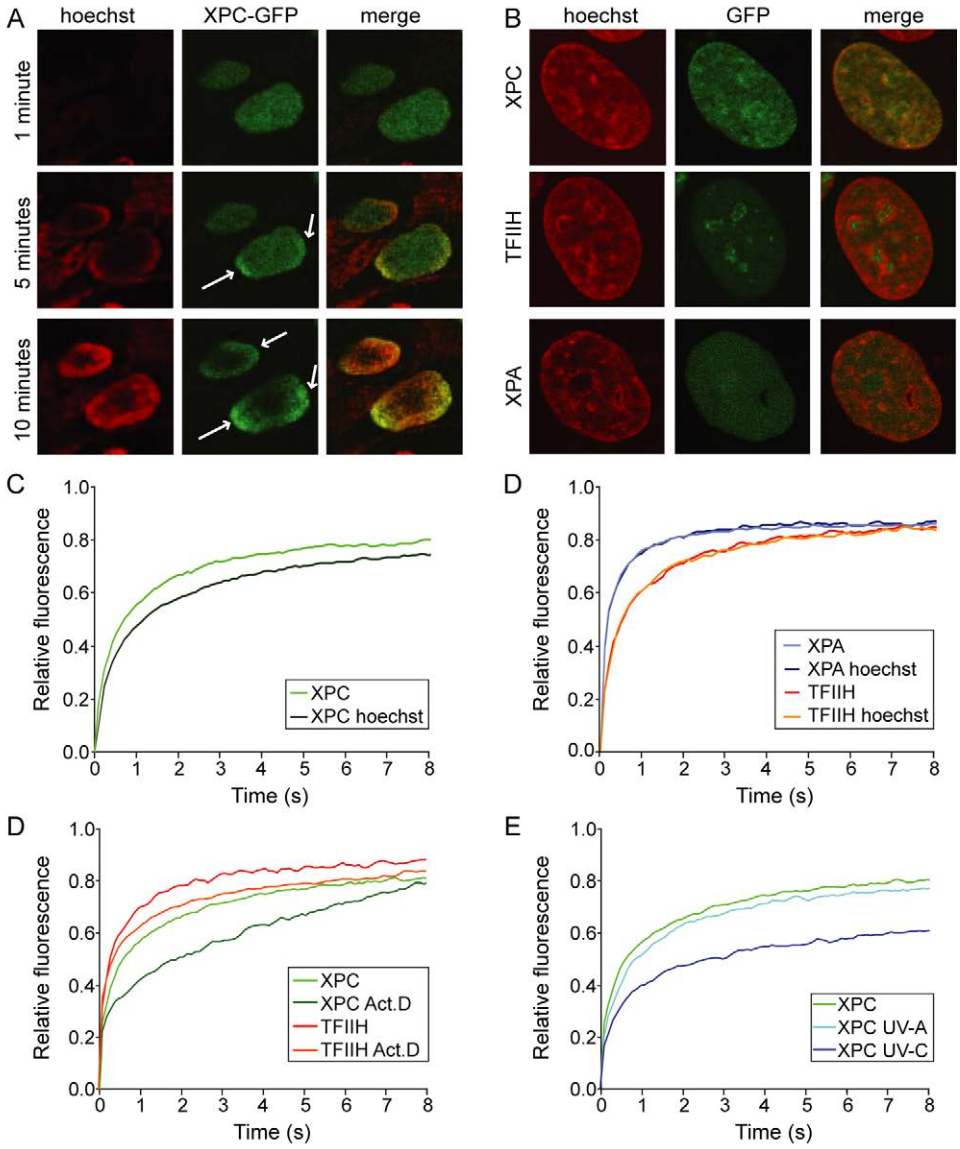

Fig. 3. Effect of DNA-structure-altering agents on XPC-GFP mobility. (A) Monitoring of the uptake of Hoechst 33342 by cells expressing XPC-GFP at different time points. Left panel, Hoechst 33342 staining of DNA; Middle, GFP-fluorescence; right, merged image. (B) Confocal images of a cell expressing XPC-GFP (upper panel), XPB-GFP (middle panel) or GFP-XPA (lower panel) stained with Hoechst 33342 for 30-60 minutes prior to fixation. Left panel, Hoechst staining of DNA; middle, GFP-fluorescence; right, merged image. (C) Strip-FRAP analysis of untreated (light green line) and Hoechst-33342-treated (dark green line) XPC-GFP-expressing cells. (D) Strip-FRAP analysis of untreated (light line) and Hoechst-33342-treated (dark line) cells expressing XPB-GFP (red lines) and GFP-XPA (blue lines). (E) Strip-FRAP analysis of untreated (light line) and actinomycin-D-treated (dark line) cells expressing XPB-GFP (red lines) and GFP-XPC (green lines). (F) Strip-FRAP analysis of untreated (green line), UV-A (light blue line) and UV-C-treated (dark blue line) XPC-GFP-expressing cells.

However, transcription inhibition using various inhibitors did not influence the mobility of XPC-GFP (Fig. 3E) nor did ATP depletion (Fig. 3F). XPC FRAP/FLIP data fitted best to curves generated by Monte Carlo simulations (Houtsmuller et al., 1999), in which a somewhat larger fraction than found in the strip-FRAP experiments (~70%) was transiently immobilized for approximately 500 mseconds at 37°C and approximately 2 seconds at 27°C. These data suggest that mobility of XPC-GFP when little or no DNA damage is present is slowed down by very transient, temperature-sensitive binding events to nuclear immobile structures, most likely to chromatin. Lower temperatures probably reduce the internal thermal molecular vibrations of the protein-DNA interface causing increased or stabilized binding.

Mobility of mutant XPC-GFP

To further investigate whether DNA probing did indeed determine the slow mobility of XPC, we studied the dynamics of a mutant XPC, deficient in in vitro DNA binding. Maillard and co-workers (Maillard et al., 2007) recently showed that nonpaired single-strand regions of DNA are mainly detected by two aromatic residues (W690 and F733) in XPC. In a naturally occurring XPC variant, tryptophan (W690) is substituted for serine (W690S), and this substitution was found to be the causative mutation in one patient (Chavanne et al., 2000). Equilibrium binding studies on defined substrates using a series of designed XPC mutants showed that the W690S XPC mutant had lost most of its affinity for ssDNA (Maillard et al., 2007), confirming earlier observations of reduced DNA-binding affinity of an XPC C-terminal fragment harboring this mutation (Bunick et al., 2006). We expressed this mutant XPC, tagged with GFP, in the same host cells as used for studying the GFP-tagged wild-type form of XPC, and determined its mobility (supplementary material Fig. S1). The mobility of this mutant was significantly enhanced compared with the wild-type XPC-GFP. Together, these data strongly support the hypothesis that the relatively slow mobility of XPC in vivo is caused by continuous binding to and dissociation from DNA.

Effect of various DNA altering agents on XPC-GFP mobility

We hypothesized that in the absence of UV damage, the mobility of XPC, which is slower than expected for a freely mobile protein

of its size, is reduced because of highly frequent very short DNA-binding events, which probe the DNA for damage. To test this hypothesis, we treated the XPC-GFP-expressing cells with different agents that affect DNA structure nonspecifically, but do not induce NER, and subsequently determined the effect on XPC-GFP mobility. We first tested the addition of the minor-groove-binding fluorescent dye Hoechst 33342 (Portugal and Waring, 1988), which allowed us to simultaneously monitor the nuclear uptake of this drug and the effect on XPC-GFP in real time (Fig. 3A). Recently, we identified that this drug induces different types of DNA lesions when photoactivated by irradiation at 405 nm (Dinant et al., 2007). Within 5 minutes of addition of Hoechst 33342, the nuclear periphery became fluorescent with a gradual decrease towards the nuclear interior, reflecting its slow penetration in live nuclei. Strikingly, XPC-GFP also accumulated at areas of high local Hoechst-stained DNA and this accumulation followed the same kinetics as nuclear uptake of the stain (Fig. 3A, and 3B, upper panel). After longer incubation with Hoechst 33342, XPC at steady state is concentrated into areas with high Hoechst signal (Fig. 3B) (i.e. heterochromatic areas; causing an even more pronounced XPC localization in these regions than without Hoechst 33342), whereas the distribution of TFIIH and XPA was not altered by Hoechst 33342 (Fig. 3B). FRAP experiments showed that the mobility of XPC-GFP (Fig. 3C), but not of GFP-XPA and TFIIH-GFP (Fig. 3D), was reduced by the addition of Hoechst 33342. In addition, the intercalating agent, actinomycin D (ActD) (Sobell, 1974) had a similar effect on the nuclear mobility of XPC-GFP, and in this case also on TFIIH-GFP (Fig. 3E) but not on GFP-XPA (data not shown) (Giglia-Mari et al., 2006). These experiments suggest that distortion of the DNA helix by binding of Hoechst 33342 or ActD induces enhanced binding of XPC-GFP and that the overall slow mobility of XPC-GFP is probably derived from nonspecific association with DNA or irregularities in DNA structure in unchallenged cells. This notion was further corroborated by treating the cells with other DNA-damaging agents that do not induce NER (such as γ-irradiation, which induces single- and double-stranded breaks, the alkylating agent methyl-methane-sulfonate and UV-A irradiation, which induces mainly oxidative base damages), which all affected the XPC-GFP mobility to a variable degree (Fig. 3F, and data not shown). Treatment with UV-C had the largest effect on the mobility of XPC-GFP (Fig. 3F). These findings provide in vivo evidence that XPC senses a much broader spectrum of conformational DNA/chromatin alteration than the lesions repaired by NER and further support a model in which XPC mobility is for a large part determined by a continuous binding to and dissociation from genomic DNA.

The fact that subtle conformational alterations of the DNA structure, for example by intercalation, retarded overall XPC nuclear mobility in vivo is in line with previous in vitro binding studies showing that XPC binds to a broad spectrum of aberrant DNA structures, which disrupts the normal B-form DNA (Kusumoto et al., 2001; Sugasawa et al., 1998; Sugasawa et al., 2001) but does not induce in vitro NER (Sugasawa et al., 2001; Sugasawa et al., 2002). These data suggest that although XPC is the main initiator of GG-NER, its association with DNA-aberrations does not always trigger productive NER. Based on these observations Dip and Sugasawa (Dip et al., 2004; Sugasawa et al., 2001) postulated a multi-step NER-licensing model, in which different aspects of distorting lesions in DNA are successively verified. This sophisticated recognition mechanism ensures a high safety level within the GG-NER pathway by allowing the NER reaction to proceed only when a NER-specific lesion is present, thereby preventing spurious and undesired incisions. Recently, in a study on the association dynamics of TTDA to TFIIH we provided evidence that in addition to XPA, TFIIH probably also has an important role in damage verification (Giglia-Mari et al., 2006).

In addition, binding of XPC to lesions other than NER-specific lesions may stimulate other damage systems, such as base excision repair (BER): XPC interacts with and stimulates enzymatic activity of 3-methyladinine DNA glycosylase (Miao et al., 2000) and thymine DNA glycosylase (Shimizu et al., 2003) and acts as a cofactor for 8-oxoguanine DNA glycosylase (D'Errico et al., 2006).

XPC-GFP binding to UV-induced lesions

To determine the active participation of XPC-GFP in NER we determined its mobility (as measured by FRAP) after applying different doses of a known NER-inducing DNA lesion (using UV-C) and compared this with unchallenged cells (Fig. 4A), as previously described (Hoogstraten et al., 2002; Houtsmuller et al., 1999; Rademakers et al., 2003). FRAP curves fitted best to a scenario in which transient immobilization of XPC-GFP was significantly longer compared with its immobilization in undamaged cells. The fraction of immobilized XPC-GFP molecules was proportional to the amount of induced damage (applied UV dose), with ~25% of XPC-GFP molecules immobilized at 8 J/m^2. Applying higher UV doses (up to 16 J/m^2) did not further increase the immobilized pool of XPC-GFP (Fig. 4A). It is surprising to note that with increasing substrate concentration (UV-damaged DNA) no further depletion of the free nuclear pool of XPC-GFP could be achieved. This observation can be explained when not all XPC molecules are able to bind, or when lesions are not accessible. A third explanation could be that another factor preceding XPC binding is limiting. Two hours after UV-irradiation the immobilized fraction was already significantly decreased (in a dose-dependent fashion) and virtually reduced to background levels at 4 hours post UV irradiation (Fig. 4B). This relatively fast reduction of immobilized XPC has also been observed for ERCC1, TFIIH and XPG (Hoogstraten et al., 2002; Houtsmuller et al., 1999; Zotter et al., 2006) and further supports the notion that with this procedure, the early robust NER response (i.e. removal of 6-4PPs) is predominantly monitored and that the relatively slower repair of CPD lesions is close to the limit of detection.

The dose-dependent immobilization of XPC-GFP in combination with the time-dependent decay of immobilization suggests that this immobilization of XPC-GFP reflects the binding of this protein into NER complexes (DNA lesion or repair factor complexes).

Binding kinetics of XPC-GFP in NER complexes

To determine the binding kinetics of XPC-GFP with DNA lesions and or NER complexes, we measured the residence time of XPC-GFP at locally damaged areas by applying simultaneous FRAP and FLIP on the accumulated XPC-GFP (Hoogstraten et al., 2002; Rademakers et al., 2003). A strip spanning the entire nucleus and covering half of the locally damaged site was bleached (Fig. 4C,D). Subsequently, the fluorescence at the bleached (FRAP) and non-bleached area (FLIP) of the local damage was monitored. The difference in relative fluorescence between the FRAP and FLIP area of the local damage was then plotted against time (Fig. 4E). The time required to obtain 90% redistribution of bleached and unbleached molecules ($t_{0.9}$) was used as a measure of the residence time of XPC-GFP molecules at NER sites. The measured $t_{0.9}$ of ~100 seconds (Fig. 4F), suggests a residence time of ~1-2 minutes,

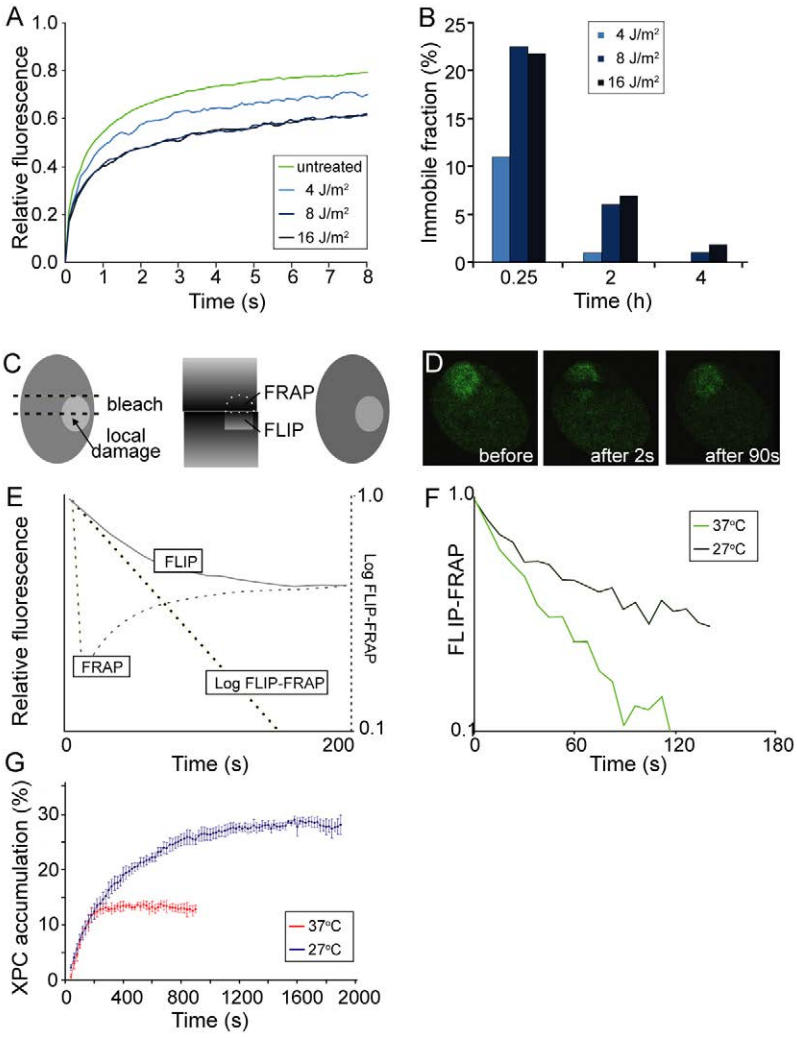

Fig. 4. FRAP analysis of UV-C-treated cells expressing XPC-GFP. (A) FRAP analysis of untreated (green line) and UV-irradiated cells (blue lines) at different UV doses. (B) UV-dose-dependent and time-dependent immobilization of XPC-GFP. Percentage of UV-induced immobilization is plotted against time for the different UV-doses, non-damage-induced immobilization was set at zero. (C) Scheme of the FRAP-FLIP procedure on locally damaged areas. A small strip covering half of the local damage and spanning the entire nucleus is bleached at relatively low laser intensity for a period of 2 seconds. Subsequently fluorescence is monitored at regular time intervals in the bleached (FRAP) and non-bleached (FLIP) half of the local damage. (D) Confocal images of a locally irradiated cell expressing XPC-GFP (5 μm pore filter). Left panel, before bleaching; middle panel, directly after bleaching and right panel, 90 seconds after bleaching. (E) The relative fluorescence of the FRAP and FLIP area is shown over time. The log of fluorescence redistribution difference between FLIP and FRAP areas are plotted against time (dotted line). (F) Simultaneous FRAP/FLIP analysis of local damage at 37°C and 27°C. (G) Assembly kinetics of XPC-GFP to locally damaged areas at 37°C and 27°C. The curves are normalized to the bound fraction in the locally damaged area.

which is significantly shorter than the binding times of the other NER factors; XPA, TFIIH, ERCC1/XPF and XPG resided at damage sites at around 4 to 6 minutes (Hoogstraten et al., 2002; Rademakers et al., 2003; Zotter et al., 2006). XPC binds around four times faster than DDB2 (Luijsterburg et al., 2007).

When the FRAP experiments were performed at 27°C, a significantly longer residence time of XPC-GFP at the locally damaged site was observed (Fig. 4F). Note that the 90% redistribution took too long to be able to accurately measure binding time at this temperature. In addition, the amount of accumulated XPC-GFP molecules in the damaged area was greatly increased compared with that at 37°C. At 37°C, XPC-GFP incorporation into NER complexes reached a steady state within ~4 minutes ($t_{1/2}$ of 100 seconds Fig. 4G). Interestingly, at 27°C, the assembly rate of XPC-GFP onto NER lesions was not affected, whereas the time to reach steady state was substantially extended to ~20 minutes ($t_{1/2}$ of 200s; Fig. 4G). This can be explained by a mechanism in which the dissociation, but not the association (similar initial slope at different temperatures) with DNA and damaged DNA depends on temperature, resulting in a higher steady-state level at locally damaged DNA (Fig. 4G).

Dynamic shuttling of XPC-GFP between nucleus and cytoplasm

Both the amount and the activity of XPC are tightly regulated at different levels: a p53-dependent transcriptional regulation (Adimoolam and Ford, 2002), RAD23-dependent and damage-induced stabilization of XPC protein (Lommel et al., 2002; Ng et al., 2003). However, both of these regulatory mechanisms are slow, yielding the highest UV-dependent XPC induction at time points when the majority of the lesions are already removed. This relatively slow damage-induced adaptive response suggests that this process mainly serves to prepare cells to respond more quickly to a possible subsequent large genotoxic attack. Recently, a new and faster mode of regulating XPC action was discovered: after DNA damage, XPC becomes quickly ubiquitylated in a DDB2 (XPE)-dependent fashion (Sugasawa et al., 2005; Wang et al., 2005). This post-translational modification probably enhances the affinity of XPC for damaged DNA and thus reflects an adaptive response that directly regulates NER activity.

Close inspection of the primary sequence of the XPC polypeptide revealed the presence of four evolutionarily conserved potential nuclear export signals (Fig. 5A,B), suggesting that XPC might be exported to the cytoplasm similarly to a number of other nuclear proteins whose concentration is tightly regulated, such as p53 (Roth et al., 1998) and some of the clock proteins (Tamaru et al., 2003; Yagita et al., 2002). To test whether XPC-GFP does shuttle between cytoplasm and nucleus in living cells, we bleached one nucleus of polynucleated cells (generated by Sendai-virus-mediated cell fusion) expressing XPC-GFP and subsequently monitored the fluorescence recovery in the bleached nucleus (Fig. 5C). We found a fluorescence recovery of 12% of the original fluorescence level in the bleached nucleus within 25 minutes, i.e. the longest time monitored (Fig. 5D, light green line). The majority of this fluorescence recovery is not derived from de novo synthesized XPC-GFP because when both nuclei were bleached, hardly any fluorescence recovery was observed (Fig. 5D, dark green line). Note that the steady-state level of XPC-GFP in the cytoplasm is very low, since imaging revealed only a slightly above-background-level of fluorescence. In similar experiments using fused cells that express TFIIH-GFP or GFP-XPA [both also mainly

visible in nuclei of living cells (Hoogstraten et al., 2002; Rademakers et al., 2003)], we did not find any significant fluorescence recovery after bleaching one nucleus (Fig. 5E), suggesting that nuclear-cytoplasmic shuttling is not a common feature of NER factors. The shuttling behavior of XPC-GFP is strongly reduced in UV-irradiated (8 J/m^2) cells (Fig. 5F, blue lines). Similar results were obtained with endogenously expressed XPC when wild-type and XPC-deficient human fibroblasts were fused. XPC protein redistribution into the previous XPC-devoid nucleus (derived from the XP-C cells) was greatly retarded after UV irradiation when compared with that in undamaged cells as detected by immunofluorescent labeling (data not shown).

Discussion

Here we analyzed the spatiotemporal distribution of XPC, the main DNA-damage sensor within GG-NER by expressing GFP-tagged XPC in human fibroblasts. The GFP-tagged XPC appeared fully functional in DNA repair when expressed at physiologically relevant levels (Fig. 1), indicating that these cells are a bona fide source to study its dynamic behavior.

Three different spatiotemporal properties distinguish XPC from the other NER proteins tested: (1) nonhomogenous nuclear distribution of XPC in living cells in which high local concentrations of XPC coincide with high local DNA concentrations; (2) colocalization of XPC with highly condensed metaphase chromosomes; (3) a surprisingly slow mobility of XPC was observed with different photobleaching (FRAP) experiments, when compared with previously tested NER factors and considering its molecular size. This latter property suggests that XPC does not freely move through the nucleoplasm. Indeed, FRAP curves fitted best to Monte-Carlo-simulated FRAP curves, in which a large fraction of ~50% of the molecules transiently (less than 1 second) interacted with a relative static component.

We propose a model in which the relative slow mobility of XPC is explained by a continuous probing (binding and subsequent dissociation) of XPC molecules to DNA or chromatin (see also Fig. 6), based on its well-established high DNA-binding affinity. This model was further substantiated by the notion that several factors that influenced the physico-chemical constitution of the chromosomal DNA, decrease the mobility of XPC even further, which is in line with increased affinity of XPC to damaged DNA (Sugasawa et al., 2001). The significantly higher mobility of a specific XPC point mutant, known to interfere with its DNA binding (Maillard et al., 2007), further corroborates this hypothesis.

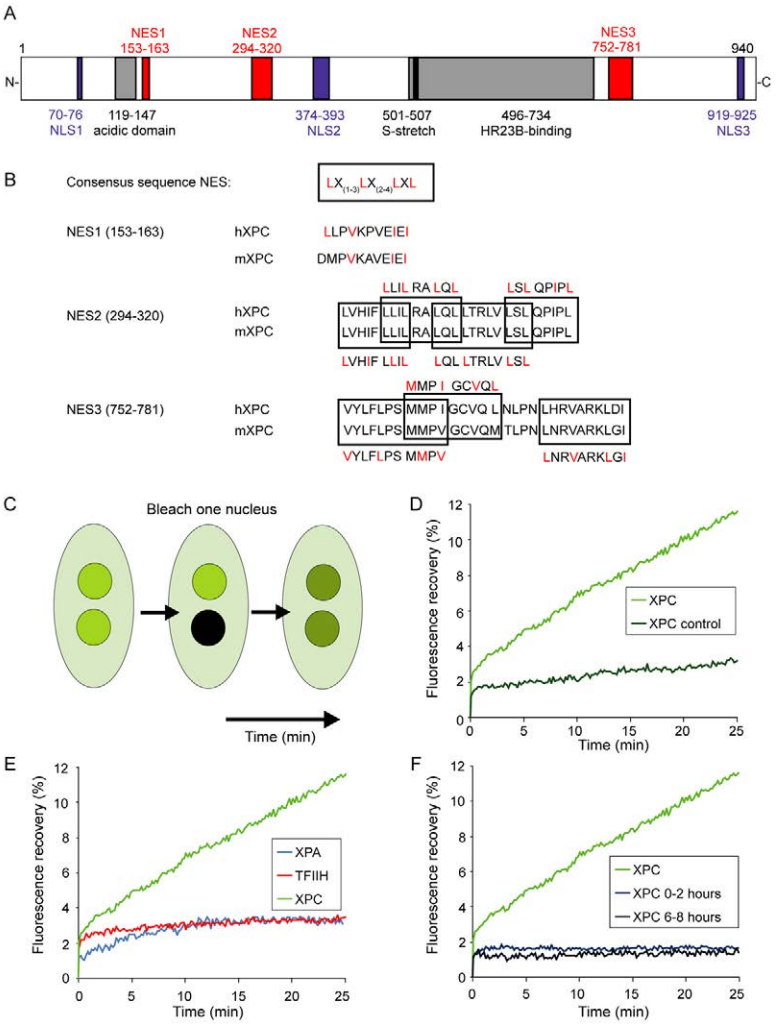

Fig. 5. Shuttling of XPC-GFP between nucleus and cytoplasm. (A) Schematic representation of the XPC polypeptide, showing the different domains. (B) The three potential NES sequences present in XPC. (C) One nucleus of the polykaryon is bleached and subsequently the fluorescence in the bleached nucleus is followed over time. (D) The relative fluorescence of XPC-GFP in the bleached nucleus over time (light green line). For the control experiment, both nuclei are bleached (dark green line). (E) The relative fluorescence of XPC-GFP (green line), XPB-GFP (red line) and GFP-XPA (blue line) in the bleached nucleus over time. (F) The relative fluorescence of XPC-GFP in the bleached nucleus in untreated (green line) cells and in cells at different time points after UV irradiation of the entire cell population (blue lines).

Dynamic association of XPC with NER complexes

We observed a UV-dose-dependent immobilization of XPC that gradually decreases in time after UV irradiation. Immobilization suggests actual binding of this damage sensor to DNA lesions and allowing NER complex assembly. We noted a shorter binding of XPC within NER-DNA lesion complexes when compared with previously tested NER factors. These observations support a scenario in which XPC dissociates from the DNA-NER protein complex before repair of a lesion is finished and support previous in vitro experiments on naked DNA (Riedl et al., 2003; Wakasugi and Sancar, 1998; You et al., 2003). Mathematical modeling suggested that the early departure of XPC from the NER complex could be beneficial for the repair efficiency (Politi et al., 2005). We favor a model in which XPC as the main initiator of GG-NER binds to a short stretch of ssDNA introduced in the opposite strand by helix-destabilizing lesions, thereby creating a good substrate for the factors, TFIIH, XPA and RPA, to bind and to further probe the lesion, allowing assembly of the incision factors. In this scenario, XPC probably leaves the pre-incision complex soon after arrival and further helical unwinding by TFIIH.

A complex multifaceted regulation mechanism of XPC

As a DNA-damage detector with binding properties for undamaged DNA, it is likely that XPC is kept under tight control. Several regulation mechanisms have been identified that influence either

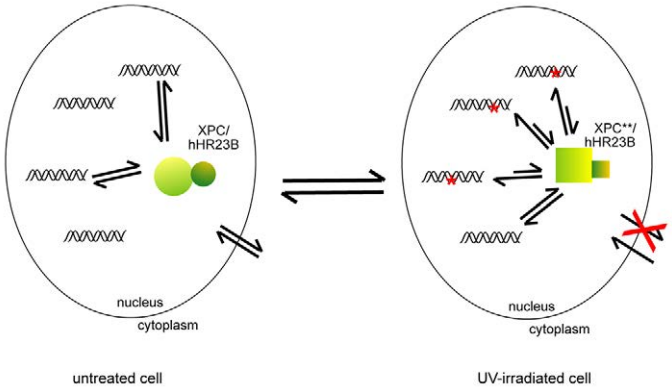

Fig. 6. Proposed model for XPC-GFP behavior in living cells. In nonirradiated cells, XPC constantly shuttles between nucleus and cytoplasm. In the nucleus, it interacts very transiently with DNA. In UV-irradiated cells, the shuttling is stopped, increasing the concentration in the nucleus. In addition, XPC continues probing DNA. Once damage is encountered, the binding time increases considerably, probably because of stabilization of the DNA-protein complex by binding of subsequent NER factors such as TFIIH and XPA.

expression at the transcriptional level (Adimoolam and Ford, 2002) or the DNA-binding properties by post-translational modification (Sugasawa et al., 2005; Wang et al., 2005). As three potential nuclear export signals (NES) in combination with three potential nuclear location signals (NLS) were identified in the primary amino acid sequence of XPC, we tested another possible mode of regulating XPC: dynamic shuttling of XPC over the nuclear membrane. We observed a differential damage-regulated nuclear-cytoplasmic shuttling of XPC, probably defining a further sophistication of the intricate XPC regulation network. Although the majority of the resident XPC molecules are located in the nucleus, the shuttling equilibrium reduces the steady-state pool of active XPC. Shuttling of XPC to the cytoplasm might also be required to reset or activate/deactivate the protein. Under normal (non-genotoxic stress) conditions, XPC continuously shuttles between the nucleoplasm and cytosol controlled by the balance between the activity of the nuclear export signals and nuclear localization signals that are present in the XPC polypeptide. These observations suggest that constitutively high levels of active XPC are unfavorable for cells, perhaps because of its continuous DNA probing, which may interfere with essential DNA transactions. The UV-induced shift towards a higher concentration of activated XPC in nuclei permits a quick response (adaptation) to changing environmental conditions.

Remarkably, XPC-GFP shuttling is still impeded 6-8 hours after UV irradiation, when the majority of XPC molecules are not involved in NER anymore (Fig. 4B). This observation argues against entrapment of XPC-GFP in the nucleus at actual NER sites as a possible explanation for the reduced recovery, but rather suggests a UV-induced modification of XPC. Rationally, the enhanced nuclear retention of XPC seems to continue too long, since at this time point the bulk of the 6-4PP lesions are removed and NER slowly progresses to remove the poorly recognized CPD lesions (Mitchell et al., 1985). A possible explanation is that a higher XPC concentration enhances the probability of locating CPD lesions in the genome because XPC does not have very high affinity for these injuries (Kusumoto et al., 2001). The mechanism responsible for nuclear retention is currently not known. It is tempting to speculate that UV-induced post-translational modifications cause this phenomenon, a likely candidate for this modification is of course the recently observed polyubiquitylation and sumoylation upon UV irradiation (Sugasawa et al., 2005; Wang et al., 2005).

In conclusion, we found that XPC has an exceptionally low mobility because of multiple transient interactions with genomic DNA. In this manner, the XPC complex 'scans' DNA in search for distortions (Fig. 6). When encountering a lesion the protein changes its conformation and aromatic residues stack with unpaired nucleotides opposite the lesion (Maillard et al., 2007; Min and Pavletich, 2007), thereby increasing its affinity and at the same time creating a protein-DNA conformation that is permissive for interaction with subsequent NER factors, probably TFIIH. Genomic insults that do not induce NER are however also sensed by XPC, as shown by decreased mobility when cells were treated with a large variety of DNA-damaging agents. Only when a bona fide NER lesion is encountered by XPC and checked by its successor(s) (TFIIH, XPA) is a functional NER complex assembled. In addition, XPC is prevented from shuttling to the cytoplasm and maintained in the nucleus up to several hours after UV irradiation. Thus, as the initiator of the NER reaction, XPC also seems to be the focal point of regulation, which probably controls the entire reaction.

Materials and Methods

Cell culture conditions and specific treatments

Cell strains used were XP4PA SV stably expressing XPC-GFP, XPCS2BA SV stably expressing XPB-GFP (Hoogstraten et al., 2002), XP2OS SV stably expressing GFP-XPA (Rademakers et al., 2003). All cell strains used in this study were cultured in RPMI + HEPES (Life Technologies) supplemented with 10% fetal calf serum and antibiotics, and maintained in a humidified 5% CO_2, 37°C incubator. For DNA staining, cells were incubated with 10 μg/ml Hoechst 33258 for 2 hours. Prior to UV irradiation with a Philips TUV lamp (254 nm) at a dose rate of ~ 0.8 J/m^2/second, cells were rinsed with PBS. In the cases when cells are locally damaged, an isopore polycarbonate filter (Millipore) containing either 5- or 8-μm-diameter pores was used to cover the cells before UV irradiation (Mone et al., 2001; Volker et al., 2001). After irradiation, cells were replaced in medium and microscopically examined.

Generation and expression of XPC-GFP-his$_6$HA fusion construct

Full-length human XPC cDNA was cloned in frame in an eukaryotic expression vector pEGFP-N3 (Clonetech). A 3′ histidine$_6$-hemagglutinin tag was added by insertion of a double-stranded oligo in *Ssp*BI-*Not*I site. The W690S mutation was introduced into wild type XPC-GFP cDNA fusion construct by site-directed mutagenesis. The XPC-GFP fusion construct was transfected to XP4PA SV cells and the cells were selected with 250 μg/ml G418 (Sigma). A UV-resistant population that survived three UV exposures (4 J/m^2) was isolated.

Confocal microscopy

Three days prior to microscopic experiments, cells were seeded onto 24-mm-diameter coverslips. Imaging and FRAP were performed on a Zeiss confocal laser-scanning microscope LSM510 meta (Zeiss, Jena, Germany), equipped with a heatable scan stage. Images were recorded with a 488nm Ar-laser and a 515-540 nm bandpass filter. Lateral resolution was 104 nm.

Fluorescence recovery after photobleaching

Mobility measurements were performed by FRAP at high time resolution (strip-FRAP) and complemented with an alternative lower time resolution combined FRAP and FLIP approach. For strip-FRAP, a narrow (~ 1 μm) strip spanning the width of the nucleus was photobleached for 63 mseconds at 100% laser intensity. Recovery of fluorescence in the strip was subsequently monitored with 21 msecond intervals at 1% laser intensity. In simultaneous FRAP-FLIP experiments, a strip at one side of a nucleus was bleached at 20% laser intensity for 8 seconds. Fluorescence was then monitored in the bleached strip (FRAP) and a corresponding strip (FLIP) at the opposite of the nucleus at constant distance and 4 second time intervals and the normalized difference between FLIP and FRAP was plotted against time (Houtsmuller and Vermeulen, 2001) (Fig. 5C).

FLIP on polykaryon cells

XPC-GFP-expressing cells were fused using 500 HAU of Sendai virus. Three days after fusion, one nucleus of a polykaryon was completely bleached using relatively low laser intensity for a period of 4 seconds (Fig. 5C). Subsequently the fluorescence

in the bleached nucleus was monitored at regular time intervals (every 10 seconds). The fluorescence regain (relative fluorescence) in the bleached nucleus was plotted against time (minutes).

FRAP data analysis

For the model-based analysis of the FRAP data, raw FRAP curves were normalized to pre-bleach values and the best fitting curve (by ordinary least squares) was picked from a large set of computer-simulated FRAP curves (generated as described below) in which three parameters representing mobility properties were varied: diffusion rate (ranging from 0.04 to 25 μm^2/second), immobile fraction (ranging from 0-90%), and time spent in immobile state (ranging from 0.1 to 300 seconds).

The Monte Carlo computer simulations used to generate FRAP curves for the fit were based on a model that simulates diffusion of molecules and binding to immobile elements in an ellipsoidal volume. The laser bleach pulse was simulated based on experimentally derived 3D laser intensity profiles, which were used to determine the probability for each molecule to get bleached considering their 3D position. The simulation of the FRAP curve was then run using discrete time steps corresponding to the experimental scan interval of 21 mseconds. Diffusion was simulated at each new time step $t + \Delta t$ by deriving the new positions ($x_{t+\Delta t}$, $y_{t+\Delta t}$, $z_{t+\Delta t}$) of all mobile molecules from their current positions (x_t, y_t, z_t) by $x_{t+\Delta t}=x_t + G(r_1)$, $y_{t+\Delta t}=y_t + G(r_2)$, and $z_{t+\Delta t}=z_t + G(r_3)$, where r_i is a random number ($0 \leq r_i \leq 1$) chosen from a uniform distribution, and $G(r_i)$ is an inversed cumulative Gaussian distribution with $\mu=0$ and $\sigma^2=6D\Delta t$, where D is the diffusion coefficient. Immobilization was derived from simple binding kinetics described by: $k_{on}/k_{off}=F_{imm} / (1–F_{imm})$, where F_{imm} is the relative number of immobile molecules. The probability for each particle to become immobilized (representing chromatin binding) is defined as $P_{immobilise}=k_{on}=k_{off}. F_{imm}/(1–F_{imm})$, where $k_{off}=1 / T_{imm}$, and T_{imm} is the average time spent in the immobile state. The probability to be released is given by $P_{mobilise}=k_{off}=1 / T_{imm}$. The simulated FRAP curves were generated by counting the number of unbleached molecules in the bleached strip at every unit time step. For FRAP-FLIP experiments unbleached molecules were counted every 4 seconds (190 time steps in the simulations) in both FRAP and FLIP areas.

Recruitment of XPC-GFP to locally irradiated cells

Cells were grown in glass bottomed dishes (MatTek, Ashland, MA) and locally UV irradiated with a UV source containing four UV lamps (Philips TUV 9W PL-S) above the microscope stage as described previously (Mone et al., 2004; Politi et al., 2005; Zotter et al., 2006). Briefly, XPC-GFP-expressing cells were locally UV irradiated through a polycarbonate mask (Millipore Billerica, MA) with pores of 5 μm (Mone et al., 2001) on a Zeiss Axiovert 100 M microscope (Zeiss, Oberkochen, Germany). The UV dose rate was 3 J/m^2/second at 254 nm as measured with an SHD 240/W detector connected to an IL 1700 radiometer (International Light Technologies, Peabody, MA), and cells were irradiated for 39 seconds (resulting in 100 J/m^2). Immediately after irradiation, the accumulation of XPC-GFP was monitored with regular time intervals (20 seconds) up to 20 minutes. Accumulation after local irradiation was quantified with Object-Image software (Vischer et al., 1999). Time courses were normalized with respect to the bound fraction in locally damaged areas. Start of the UV irradiation was defined as t=0.

The authors thank N. G. J. Jaspers and T. G. J. van der Horst for helpful discussions. This work was supported by the Dutch Organisation for Scientific Research (NWO): ZonMW 912-03-012, 917-46-371, 917-46-364; 901-01-229; ESF, Eurodyna 855-01-072; EU FP6 LSHG-CT-2005-512113; HFSP RGP0007/2004-C; AICR 05-045 and INTAS 06-1000013-9210.

References

Adimoolam, S. and Ford, J. M. (2002). p53 and DNA damage-inducible expression of the xeroderma pigmentosum group C gene. *Proc. Natl. Acad. Sci. USA* **99**,12985-12990.

Alekseev, S., Kool, H., Rebel, H., Fousteri, M., Moser, J., Backendorf, C., de Gruijl, F. R., Vrieling, H. and Mullenders, L. H. (2005). Enhanced DDB2 expression protects mice from carcinogenic effects of chronic UV-B irradiation. *Cancer Res.* **65**, 10298-10306.

Batty, D., Rapic'-Otrin, V., Levine, A. S. and Wood, R. D. (2000). Stable binding of human XPC complex to irradiated DNA confers strong discrimination for damaged sites. *J. Mol. Biol.* **300**, 275-290.

Bunick, C. G., Miller, M. R., Fuller, B. E., Fanning, E. and Chazin, W. J. (2006). Biochemical and structural domain analysis of xeroderma pigmentosum complementation group C protein. *Biochemistry* **45**, 14965-14979.

Buterin, T., Meyer, C., Giese, B. and Naegeli, H. (2005). DNA quality control by conformational readout on the undamaged strand of the double helix. *Chem. Biol.* **12**, 913-922.

Chavanne, F., Broughton, B. C., Pietra, D., Nardo, T., Browitt, A., Lehmann, A. R. and Stefanini, M. (2000). Mutations in the XPC gene in families with xeroderma pigmentosum and consequences at the cell, protein, and transcript levels. *Cancer Res.* **60**, 1974-1982.

Chen, D., Dundr, M., Wang, C., Leung, A., Lamond, A., Misteli, T. and Huang, S. (2005). Condensed mitotic chromatin is accessible to transcription factors and chromatin structural proteins. *J. Cell Biol.* **168**, 41-54.

Chu, G. and Chang, E. (1988). Xeroderma pigmentosum group E cells lack a nuclear factor that binds to damaged DNA. *Science* **242**, 564-567.

Daya-Grosjean, L., James, M. R., Drougard, C. and Sarasin, A. (1987). An immortalized xeroderma pigmentosum, group C, cell line which replicates SV40 shuttle vectors. *Mutat. Res.* **183**, 185-196.

D'Errico, M., Parlanti, E., Teson, M., de Jesus, B. M., Degan, P., Calcagnile, A., Jaruga, P., Bjoras, M., Crescenzi, M., Pedrini, A. M. et al. (2006). New functions of XPC in the protection of human skin cells from oxidative damage. *EMBO J.* **25**, 4305-4315.

Dinant, C., de Jager, M., Essers, J., van Cappellen, W. A., Kanaar, R., Houtsmuller, A. B. and Vermeulen, W. (2007). Activation of multiple DNA repair pathways by subnuclear damage induction methods. *J. Cell Sci.* **120**, 2731-2740.

Dip, R., Camenisch, U. and Naegeli, H. (2004). Mechanisms of DNA damage recognition and strand discrimination in human nucleotide excision repair. *DNA Repair (Amst.)* **3**, 1409-1423.

Garinis, G. A., Mitchell, J. R., Moorhouse, M. J., Hanada, K., de Waard, H., Vandeputte, D., Jans, J., Brand, K., Smid, M., van der Spek, P. J. et al. (2005). Transcriptome analysis reveals cyclobutane pyrimidine dimers as a major source of UV-induced DNA breaks. *EMBO J.* **24**, 3952-3962.

Giglia-Mari, G., Miquel, C., Theil, A. F., Mari, P. O., Hoogstraten, D., Ng, J. M., Dinant, C., Hoeijmakers, J. H. and Vermeulen, W. (2006). Dynamic interaction of TTDA with TFIIH is stabilized by nucleotide excision repair in living cells. *PLoS Biol.* **4**, e156.

Gillet, L. C. and Scharer, O. D. (2006). Molecular mechanisms of mammalian global genome nucleotide excision repair. *Chem. Rev.* **106**, 253-276.

Gunz, D., Hess, M. T. and Naegeli, H. (1996). Recognition of DNA adducts by human nucleotide excision repair. Evidence for a thermodynamic probing mechanism. *J. Biol. Chem.* **271**, 25089-25098.

Halford, S. E. and Szczelkun, M. D. (2002). How to get from A to B: strategies for analysing protein motion on DNA. *Eur. Biophys. J.* **31**, 257-267.

Hoogstraten, D., Nigg, A. L., Heath, H., Mullenders, L. H., van Driel, R., Hoeijmakers, J. H., Vermeulen, W. and Houtsmuller, A. B. (2002). Rapid switching of TFIIH between RNA polymerase I and II transcription and DNA repair in vivo. *Mol. Cell* **10**, 1163-1174.

Houtsmuller, A. B. and Vermeulen, W. (2001). Macromolecular dynamics in living cell nuclei revealed by fluorescence redistribution after photobleaching. *Histochem. Cell Biol.* **115**, 13-21.

Houtsmuller, A. B., Rademakers, S., Nigg, A. L., Hoogstraten, D., Hoeijmakers, J. H. and Vermeulen, W. (1999). Action of DNA repair endonuclease ERCC1/XPF in living cells. *Science* **284**, 958-961.

Janicijevic, A., Sugasawa, K., Shimizu, Y., Hanaoka, F., Wijgers, N., Djurica, M., Hoeijmakers, J. H. and Wyman, C. (2003). DNA bending by the human damage recognition complex XPC-HR23B. *DNA Repair (Amst.)* **2**, 325-336.

Kanda, T., Sullivan, K. F. and Wahl, G. M. (1998). Histone-GFP fusion protein enables sensitive analysis of chromosome dynamics in living mammalian cells. *Curr. Biol.* **8**, 377-385.

Kusumoto, R., Masutani, C., Sugasawa, K., Iwai, S., Araki, M., Uchida, A., Mizukoshi, T. and Hanaoka, F. (2001). Diversity of the damage recognition step in the global genomic nucleotide excision repair in vitro. *Mutat. Res.* **485**, 219-227.

Lommel, L., Ortolan, T., Chen, L., Madura, K. and Sweder, K. S. (2002). Proteolysis of a nucleotide excision repair protein by the 26 S proteasome. *Curr. Genet.* **42**, 9-20.

Luijsterburg, M. S., Goedhart, J., Moser, J., Kool, H., Geverts, B., Houtsmuller, A. B., Mullenders, L. H., Vermeulen, W. and van Driel, R. (2007). Dynamic in vivo interaction of DDB2 E3 ubiquitin ligase with UV-damaged DNA is independent of damage recognition protein XPC. *J. Cell Sci.* in press.

Maillard, O., Solyom, S. and Naegeli, H. (2007). An aromatic sensor with aversion to damaged strands confers versatility to DNA repair. *PLoS Biol.* **5**, e79.

Masutani, C., Sugasawa, K., Yanagisawa, J., Sonoyama, T., Ui, M., Enomoto, T., Takio, K., Tanaka, K., van der Spek, P. J., Bootsma, D. et al. (1994). Purification and cloning of a nucleotide excision repair complex involving the xeroderma pigmentosum group C protein and a human homologue of yeast RAD23. *EMBO J.* **13**, 1831-1843.

Miao, F., Bouziane, M., Dammann, R., Masutani, C., Hanaoka, F., Pfeifer, G. and O'Connor, T. R. (2000). 3-Methyladenine-DNA glycosylase (MPG protein) interacts with human RAD23 proteins. *J. Biol. Chem.* **275**, 28433-28438.

Min, J. H. and Pavletich, N. P. (2007). Recognition of DNA damage by the Rad4 nucleotide excision repair protein. *Nature* **449**, 570-575.

Mitchell, D. L., Haipek, C. A. and Clarkson,. J. M. (1985). (6-4)Photoproducts are removed from the DNA of UV-irradiated mammalian cells more efficiently than cyclobutane pyrimidine dimers. *Mutat. Res.* **143**, 109-112.

Mone, M. J., Volker, M., Nikaido, O., Mullenders, L. H., van Zeeland, A. A., Verschure, P. J., Manders, E. M. and van Driel, R. (2001). Local UV-induced DNA damage in cell nuclei results in local transcription inhibition. *EMBO Rep.* **2**, 1013-1017.

Mone, M. J., Bernas, T., Dinant, C., Goedvree, F. A., Manders, E. M., Volker, M., Houtsmuller, A. B., Hoeijmakers, J. H., Vermeulen, W. and van Driel, R. (2004). In vivo dynamics of chromatin-associated complex formation in mammalian nucleotide excision repair. *Proc. Natl. Acad. Sci. USA* **101**, 15933-15937.

Moser, J., Volker, M., Kool, H., Alekseev, S., Vrieling, H., Yasui, A., van Zeeland, A. A. and Mullenders, L. H. (2005). The UV-damaged DNA binding protein mediates efficient targeting of the nucleotide excision repair complex to UV-induced photo lesions. *DNA Repair (Amst.)* **4**, 571-582.

Ng, J. M., Vermeulen, W., van der Horst, G. T., Bergink, S., Sugasawa, K., Vrieling, H. and Hoeijmakers, J. H. (2003). A novel regulation mechanism of DNA repair by

damage-induced and RAD23-dependent stabilization of xeroderma pigmentosum group C protein. *Genes Dev*. **17**, 1630-1645.

Politi, A., Mone, M. J., Houtsmuller, A. B., Hoogstraten, D., Vermeulen, W., Heinrich, R. and van Driel, R. (2005). Mathematical modeling of nucleotide excision repair reveals efficiency of sequential assembly strategies. *Mol. Cell* **19**, 679-690.

Portugal, J. and Waring, M. J. (1988). Assignment of DNA binding sites for 4',6-diamidine-2-phenylindole and bisbenzimide (Hoechst 33258). A comparative footprinting study. *Biochem. Biophys. Acta*. **949**, 158-168.

Rademakers, S., Volker, M., Hoogstraten, D., Nigg, A. L., Mone, M. J., Van Zeeland, A. A., Hoeijmakers, J. H., Houtsmuller, A. B. and Vermeulen, W. (2003). Xeroderma pigmentosum group A protein loads as a separate factor onto DNA lesions. *Mol. Cell. Biol*. **23**, 5755-5767.

Reardon, J. T., Mu, D. and Sancar, A. (1996). Overproduction, purification, and characterization of the XPC subunit of the human DNA repair excision nuclease. *J. Biol. Chem*. **271**, 19451-19456.

Riedl, T., Hanaoka, F. and Egly, J. M. (2003). The comings and goings of nucleotide excision repair factors on damaged DNA. *EMBO J*. **22**, 5293-5303.

Roth, J., Dobbelstein, M., Freedman, D. A., Shenk, T. and Levine, A. J. (1998). Nucleo-cytoplasmic shuttling of the hdm2 oncoprotein regulates the levels of the p53 protein via a pathway used by the human immunodeficiency virus rev protein. *EMBO J*. **17**, 554-564.

Shimizu, Y., Iwai, S., Hanaoka, F. and Sugasawa, K. (2003). Xeroderma pigmentosum group C protein interacts physically and functionally with thymine DNA glycosylase. *EMBO J*. **22**, 164-173.

Sobell, H. M. (1974). The stereochemistry of actinomycin binding to DNA. *Cancer Chemother. Rep*. **58**, 101-116.

Sugasawa, K., Ng, J. M., Masutani, C., Iwai, S., van der Spek, P. J., Eker, A. P., Hanaoka, F., Bootsma, D. and Hoeijmakers, J. H. (1998). Xeroderma pigmentosum group C protein complex is the initiator of global genome nucleotide excision repair. *Mol. Cell* **2**, 223-232.

Sugasawa, K., Okamoto, T., Shimizu, Y., Masutani, C., Iwai, S. and Hanaoka, F. (2001). A multistep damage recognition mechanism for global genomic nucleotide excision repair. *Genes Dev*. **15**, 507-521.

Sugasawa, K., Shimizu, Y., Iwai, S. and Hanaoka, F. (2002). A molecular mechanism for DNA damage recognition by the xeroderma pigmentosum group C protein complex. *DNA Repair (Amst.)* **1**, 95-107.

Sugasawa, K., Okuda, Y., Saijo, M., Nishi, R., Matsuda, N., Chu, G., Mori, T., Iwai, S., Tanaka, K. and Hanaoka, F. (2005). UV-induced ubiquitylation of XPC protein mediated by UV-DDB-ubiquitin ligase complex. *Cell* **121**, 387-400.

Tamaru, T., Isojima, Y., van der Horst, G. T., Takei, K., Nagai, K. and Takamatsu, K. (2003). Nucleocytoplasmic shuttling and phosphorylation of BMAL1 are regulated by circadian clock in cultured fibroblasts. *Genes Cells* **8**, 973-983.

van den Boom, V., Citterio, E., Hoogstraten, D., Zotter, A., Egly, J. M., van Cappellen, W. A., Hoeijmakers, J. H., Houtsmuller, A. B. and Vermeulen, W. (2004). DNA damage stabilizes interaction of CSB with the transcription elongation machinery. *J. Cell Biol*. **166**, 27-36.

van der Spek, P. J., Eker, A., Rademakers, S., Visser, C., Sugasawa, K., Masutani, C., Hanaoka, F., Bootsma, D. and Hoeijmakers, J. H. (1996). XPC and human homologs of RAD23: intracellular localization and relationship to other nucleotide excision repair complexes. *Nucleic Acids Res*. **24**, 2551-2559.

Venema, J., van Hoffen, A., Natarajan, A. T., van Zeeland, A. A. and Mullenders, L. H. (1990). The residual repair capacity of xeroderma pigmentosum complementation group C fibroblasts is highly specific for transcriptionally active DNA. *Nucleic Acids Res*. **18**, 443-448.

Verschure, P. J., van der Kraan, I., Manders, E. M., Hoogstraten, D., Houtsmuller, A. B. and van Driel, R. (2003). Condensed chromatin domains in the mammalian nucleus are accessible to large macromolecules. *EMBO Rep*. **4**, 861-866.

Vischer, N. O., Huls, P. G., Ghauharali, R. I., Brakenhoff, G. J., Nanninga, N. and Woldringh, C. L. (1999). Image cytometric method for quantifying the relative amount of DNA in bacterial nucleoids using Escherichia coli. *J. Microsc.* **196**, 61-68.

Volker, M., Mone, M. J., Karmakar, P., van Hoffen, A., Schul, W., Vermeulen, W., Hoeijmakers, J. H., van Driel, R., van Zeeland, A. A. and Mullenders, L. H. (2001). Sequential assembly of the nucleotide excision repair factors in vivo. *Mol. Cell* **8**, 213-224.

Wakasugi, M. and Sancar, A. (1998). Assembly, subunit composition, and footprint of human DNA repair excision nuclease. *Proc. Natl. Acad. Sci. USA* **95**, 6669-6674.

Wakasugi, M., Shimizu, M., Morioka, H., Linn, S., Nikaido, O. and Matsunaga, T. (2001). Damaged DNA-binding protein DDB stimulates the excision of cyclobutane pyrimidine dimers in vitro in concert with XPA and replication protein A. *J. Biol. Chem*. **276**, 15434-15440.

Wakasugi, M., Kawashima, A., Morioka, H., Linn, S., Sancar, A., Mori, T., Nikaido, O. and Matsunaga, T. (2002). DDB accumulates at DNA damage sites immediately after UV irradiation and directly stimulates nucleotide excision repair. *J. Biol. Chem*. **277**, 1637-1640.

Wang, Q. E., Wani, M. A., Chen, J., Zhu, Q., Wani, G., El-Mahdy, M. A. and Wani, A. A. (2005). Cellular ubiquitination and proteasomal functions positively modulate mammalian nucleotide excision repair. *Mol. Carcinog*. **42**, 53-64.

Wang, Q. E., Praetorius-Ibba, M., Zhu, Q., El-Mahdy, M. A., Wani, G., Zhao, Q., Qin, S., Patnaik, S. and Wani, A. A. (2007). Ubiquitylation-independent degradation of Xeroderma pigmentosum group C protein is required for efficient nucleotide excision repair. *Nucleic Acids Res*. **35**, 5338-5350.

Yagita, K., Tamanini, F., Yasuda, M., Hoeijmakers, J. H., van der Horst, G. T. and Okamura, H. (2002). Nucleocytoplasmic shuttling and mCRY-dependent inhibition of ubiquitylation of the mPER2 clock protein. *EMBO J*. **21**, 1301-1314.

You, J. S., Wang, M. and Lee. S. H. (2003). Biochemical analysis of the damage recognition process in nucleotide excision repair. *J. Biol. Chem*. **278**, 7476-7485.

Zotter, A., Luijsterburg, M. S., Warmerdam, D. O., Ibrahim, S., Nigg, A., van Cappellen, W. A., Hoeijmakers, J. H., van Driel, R., Vermeulen, W. and Houtsmuller, A. B. (2006). Recruitment of the nucleotide excision repair endonuclease XPG to sites of UV-induced dna damage depends on functional TFIIH. *Mol. Cell. Biol*. **26**, 8868-8879.

Journal of Cell Science